Korean J. Chem. Eng., 39(6), 1460-1471 (2022)
DOI: 10.1007/s11814-021-1016-9

pISSN: 0256-1115
eISSN: 1975-7220

Reaction mechanism and kinetic modeling of olefin conversion over phosphorus modified ZSM-5 catalyst

Ashenafi Hailu Berta*,,‡, Ho Dong Hwang*,**,‡, Hagos Birhane Asfha*,**, Na Young Kang*, Kiwoong Kim*,†, and Yong-Ki Park*,†**

*Center for Convergent Chemical Process, Korea Research Institute of Chemical Technology (KRICT), Gajeong-ro 141, Yuseong-gu, Daejeon 34114, Korea
**Advanced Materials and Chemical Engineering, University of Science and Technology (UST), Gajeong-ro 217, Yuseong-gu, Daejeon 34113, Korea
(*Received 14 October 2021 • Revised 17 November 2021 • Accepted 17 November 2021*)

Abstract−Reaction pathways and kinetics of C_2-C_6 olefins cracking over ZSM-5 catalyst were investigated based on product distribution to develop a model. Experimental tests of the catalytic cracking of olefins were performed in the temperature range of 450-650 °C, space-time of 0.375-3.5 min, and partial pressure of 0.08-0.23 atm. For each feed, a possible reaction pathway was identified and used for the model. Based on the identified reactions a lumped kinetic model was developed using the power-law method. The developed model included direct olefin cracking, oligomerization, and re-cracking of oligomers. Thirteen reversible reactions were considered as major reactions to represent this complex system. For each forward and backward reaction step, apparent activation energy and pre-exponential factors were estimated. The model predicts the experimental product components with an R^2 value of 0.8735-0.9718. Comparison of experimental result with the developed model showed the developed model predicted the feed product distribution with accuracy. Sensitivity analysis was done to identify dominant reaction paths for each feed that affected the yield of ethylene and propylene, the main products that needed to be maximized during industrial catalytic cracking.

Keywords: Olefins, Oligomerization, β-Scission Cracking, ZSM-5 Catalyst, Kinetics, and Modeling

INTRODUCTION

Ethylene and propylene are the most useful building block chemicals in the petrochemical industry [1-5]. With the alarming rate of increasing demand, their use as a starting material for the production of a variety of products, includes, but not limited to, polymers, plastics, fibers, diapers, packaging materials, and tires. Steam cracking of hydrocarbons has been a major source of these vital light olefins. Depending on feedstock type and operating condition, the yield of ethylene and propylene varies between 24-55% and 1.5-18%, respectively [3]. Even though it is the major source of light olefins, steam cracking by itself has the following known limitations and disadvantages: limited propylene to ethylene ratio, which suffers to fulfill fast-growing propylene demand, high energy consumption due to the high operating temperature, usually above 800 °C, and global environmental issues of CO_2 emission [1,4]. Therefore, an alternative route that addresses the existing problem is needed. Catalytic cracking of hydrocarbons attracted researchers' attention to overcome these drawbacks of steam cracking. It provides desired control of the propylene to ethylene ratio and operates relatively at lower temperatures of 550-650 °C, which significantly reduces energy consumption and CO_2 emissions [3,6].

It is well known that olefins are the primary products of protolytic cracking of paraffin, which include ethylene and propylene as the most valuable products to be maximized [1,7-11]. Interconversion of C_2-C_4 olefins provides information on the interaction and stability of these important products [2,12-15]. Paraffins, in turn, are also the major components of naphtha and other feedstock which are used to produce light olefins in catalytic cracking. Therefore, a good understanding of reaction pathways and identification of major reactions in olefin cracking will not only give firsthand information for olefin cracking but also provide an insight to interpreting the product distribution of many other feeds.

But, due to the complex nature of olefins during cracking, their reaction kinetics and modeling have not been investigated as rigorously as paraffin. These complexities in olefin cracking may arise from the difficulty of obtaining lower feed conversion because olefins are highly reactive and have a lower temperature of cracking compared to paraffin [16], quantification challenge of intermediates due to the unstable nature of olefins, and the existence of many species with many reaction possibilities. Knowledge of the reaction behavior of different carbon number feeds leads to the general reaction mechanism of olefins, which later can be used to maximize desired product components by controlling working conditions [4,5,12,17-21].

To overcome these challenges, much improvement has been observed on kinetics study approaches of olefin cracking to find reaction pathways. Based on the purpose of the study, the feed can be alcohol, extract information that can be applied to methanol to olefin

†To whom correspondence should be addressed.
E-mail: kwkim@krict.re.kr, ykpark@krict.re.kr
‡Authors contributed equally to the manuscript.

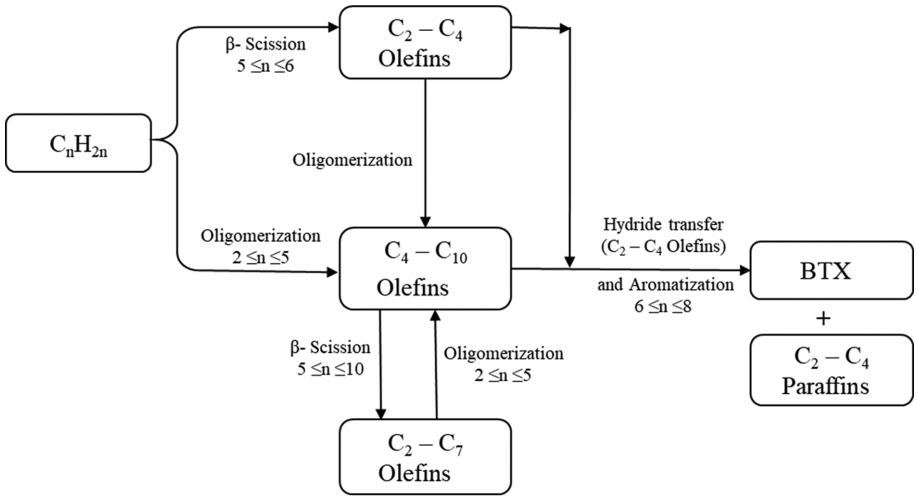

Fig. 1. Schematic diagram of catalytic cracking of olefin reactions.

study or pure olefin feed, to understand naphtha and other related feed cracking involving olefins [4]. Ying et al. [21] used C_2-C_7 pure olefin feed and power law for the reaction rate, and Huang et al. [19], used C_3-C_7 alcohol olefin feed and Langmuir Hinshelwood Hougen Watson (LHHW) for rate law, showing interconversion of olefins for the range of carbon numbers of C_2-C_7 olefins and identifying dominant reactions for different space-time and temperature to develop a model. Both of them agreed that the oligomerization reaction and β-scission cracking were dominant reactions in olefin conversion.

Most recently, Warnecke et al's work on identifying reaction pathways and kinetic modeling of olefin interconversion of C_2-C_7 olefin feed has shown a big improvement from previous work in different ways. They used mixed olefin feeds besides the usual single feed and that provided information for bimolecular reactions and gave a chance to quantify assumed intermediate higher carbon number olefins. They also used both the simple power law and Langmuir Hinshelwood Hougen Watson's (LHHW) rate law to develop a model for the identified reactions and chose the best that fits the experimental results [4]. In line with previous work, they also agreed that in olefin cracking, monomolecular β-scission cracking and bimolecular oligomerization reactions were the dominant reactions.

To avoid the complexity of the reactions, in these highly reactive catalytic crackings most of the works, if not all, did not consider aromatization reaction in their kinetic model as Ying et al. included it as a single reaction [21]. Abbot and Wojciechowski showed, on the mechanism of catalytic cracking of n-alkenes on ZSM-5 zeolite, isomerization reaction took place before monomolecular β-scission and bimolecular oligomerization reactions at a lower temperature [17]. The final product distribution depends on the type of isomer formed during the isomerization reaction step. Considering isomerization reaction in olefin cracking makes the study more difficult because when the number of carbons increases the possible isomers are too many to detect and quantify.

The other way of minimizing the complexity of reactions that causes difficulty in the kinetic study of olefin cracking is running experiments at lower temperatures and using a less acidic catalyst, a catalyst with high silicon to aluminum ratio. To that end, catalytic cracking of olefins on ZSM-5 catalyst is usually carried out below 500 °C. Though Li et al. work on Fe and P modified catalyst covering a higher temperature range of 490-610 °C for a mixed feed of butene and pentene, it is not easy to find literature for a wide range of olefin feed carried out at higher temperature [22]. To have the full picture of the actual working conditions in the industry, it is important to study cracking at higher temperature and more acidic catalyst.

This work investigated reaction pathways and developed a kinetic model for C_2-C_6 olefins feed at a temperature range of 450-650 °C over a relatively more acidic (low silicon to aluminum ratio) ZSM-5 catalyst. Each olefin feed was used as a single feed and a mixture of propylene and ethylene was also fed to analyze the stability and interaction of these important light olefins, which are needed to be maximized in catalytic cracking. For each olefin feed, a possible reaction pathway was identified based on experimental data and a kinetic model was developed by considering cracking and oligomerization reactions. From the developed model, kinetic parameters for each reaction step were determined. A schematic diagram of a possible reaction route from the observed product distribution is shown in Fig. 1.

EXPERIMENTAL

1. Catalyst Preparation and Characterization

A micro-spherical catalyst, with ZSM-5 zeolite, which was used for the catalytic cracking reaction, was prepared by spray-drying method from Albemarle Corporation (Si/Al=14.5) as the main component. Slurries containing ZSM-5, H_3PO_4, Kaolin matrix, and alumina binder were prepared by mixing thoroughly and then spray dried. The obtained micro-spherical catalyst having micron sizes was calcined at 650 °C for 6 h with air and then steamed at 760 °C for 24 hr with 100% steam for the formation of an equilibrated catalyst.

The synthesized catalyst was characterized for the confirmation

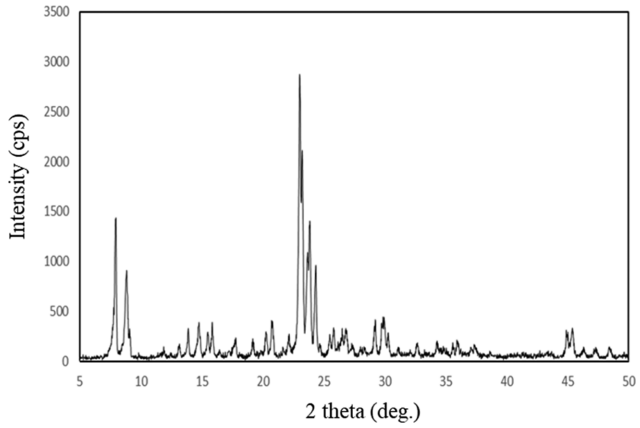

Fig. 2. XRD patterns of P-ZSM-5 zeolite.

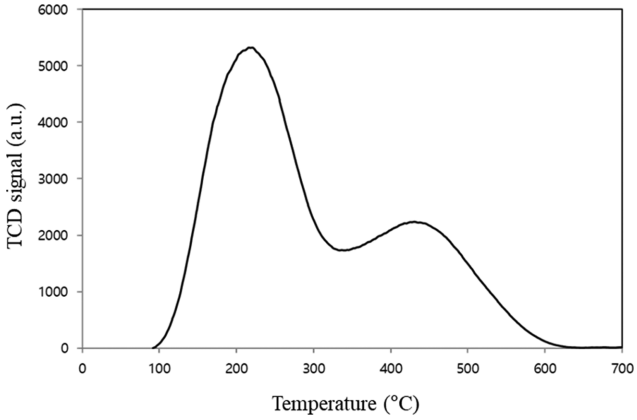

Fig. 3. NH_3-TPD profile of P-ZSM-5 zeolite.

of desired property, as shown in Table 1. Particle size analyzer to determine particle diameter, argon adsorption to determine surface area, and mercury porosimetry to determine the bulk density of the synthesized ZSM-5 catalyst were used.

XRD diffraction analysis used Rigaku Minflex model power diffractometer with analysis condition at 30 kV and 15 mA with Cu-Kα radiation (λ=1.5418 Å) and a scanning rate of 4 °Cmin^{-1} and the result shown in Fig. 2. Liu et al showed that the sharpness of the peaks of the P-ZSM-5 catalyst was decreased compared to that of the parent ZSM-5 catalyst, which indicated phosphorus modification decreased crystallinity of the zeolite catalyst to enhance the total surface area [13].

NH_3-TPD profile shown in Fig. 3 was used to determine the total acidity of the catalyst using BELCAT B. During the analysis, a 0.12 gm sample was used. The sample was heated and pretreated at 550 °C with a ramping temperature of 5 °Cmin^{-1}. After pretreatment, the sample was cooled to 100 °C for NH_3 adsorption with 30% NH_3 and helium mixture for 60 minutes. Then NH_3 desorption was measured from 100-900 °C for ramping temperature of 10 °C min^{-1}. Total areas of the peaks observed at 224 °C and 415 °C were used to determine the total acidity of the catalyst.

Table 1. A characteristic property of ZSM-5 catalyst

Property	Value
BET surface area, m^2g^{-1}	238
Particle diameter, μm	110
Total acidity, mmol g^{-1}	0.23
Bulk density, gml^{-1}	0.54

2. Experimental Setup and Chemicals

A schematic diagram of the reactor setup is presented in Fig. 4. A syringe pump and a mass flowmeter were used to control liq-

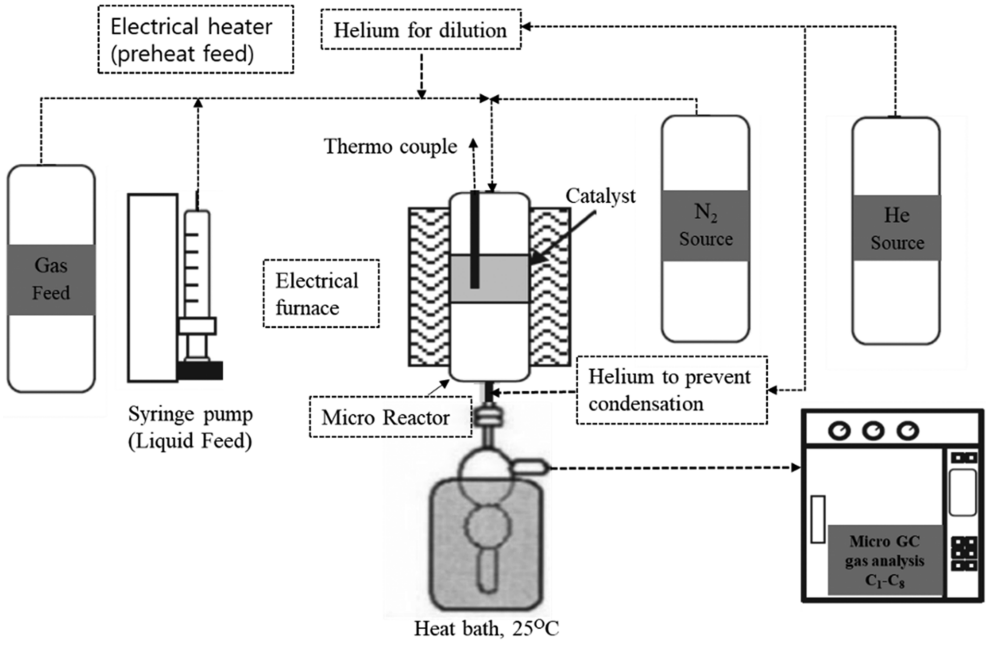

Fig. 4. Schematic diagram of experimental reactor setup.

uid and gas feed flow into the reactor, respectively. Catalytic cracking of olefin reactions was carried out in a fixed bed quartz reactor placed inside a cylindrical glass tube heated by an electrical furnace. The reactor has an internal diameter of 11.5 mm with a catalyst bed height of ~12 mm. The temperature of the furnace was controlled by a PID temperature controller. The catalyst was placed above ceramic wool support of about 5 mm and a thermocouple mounted on the catalyst surface was used to control the actual reaction temperature. Products were diluted by helium to lower partial pressure below the vapor pressure of the less volatile component to avoid condensation before analysis. Components were analyzed on-line by gas chromatography (3000 micro GC, INFICON) equipped with four separated channels and thermal conductivity detectors. The columns used in each channel were: molecular sieve for channel A to analyze methane, Plot U for channel B to analyze ethane and ethylene, alumina for channel C to analyze C_3 and C_4 components, and Ov-1 for channel D to analyze all components above C_5.

In all kinetic reactions, the synthesized ZSM-5 catalyst with a physicochemical property summarized in Table 1 was used. Liquid feeds 1-pentene (from Aldrich chemical 99% purity) and 1-hexene (Samchun chemical 97% purity) were used. For gas feeds ethylene, propylene, and 1-butene (from RIGAS, 99.5% purity) were used. Nitrogen was the standard gas for product flow quantification in GC and helium was used as a dilution of feed to adjust partial pressure of reactants and to lower partial pressure below the vapor pressure of products before analysis.

3. Olefin Cracking Reactions

Olefin cracking data was obtained for a temperature range of 450-650 °C and space-time of 0.375-3.5 min. The total pressure of the reactor for all reactions was kept atmospheric and, depending on their reactivity, partial pressure of feeds was 0.08-0.23 atm, 0.20 atm for propylene, 0.23 atm for 1-butene, 0.20 atm for 1-pentene, and 0.08 atm for 1-hexene. Nitrogen flow was kept 5 $mlmin^{-1}$ and adjustment on partial pressure was done by helium. Weight hour space velocity was varied by varying the weight of the catalyst from 12.5-50 mg for a fixed flow rate of hydrocarbon at 2 ghr^{-1}. The yield of product components, conversion of feed hydrocarbons, and molar selectivity of product components were calculated from the feed in the input stream and products and unconverted feed from the output stream.

Reactants were fed continuously to the reactor for 1 hr and 15 min and experimental results were collected from sampling and analysis of the effluent stream. For each experimental run, a fresh catalyst was used. The first sample was taken after steady-state conditions were achieved in 15 minutes of the start of the experiment and then six samples were taken in 10 minute intervals. No significant difference in product distribution was observed among samples after steady-state condition. This indicated that catalyst deactivation did not occur throughout the reaction time. The average product distribution obtained from the six samplings was taken as the final value of the run.

EXPERIMENTAL RESULT AND DISCUSSION

Reaction pathways of olefin cracking depend on the acidity of the catalyst and the molecular size of the feed. Olefin cracking undergoes mainly oligomerization and the β-scission reaction of the carbenium ion formed from the protonated olefin feed, and it is believed these reactions are dominant over other reactions [12,13, 17-21]. Isomerization of the feed plays an important role to determine product distribution and aromatization reaction at higher temperatures cannot be ignored [17,18,23]. For specified catalysts of interest, reaction pathways are greatly influenced by operating conditions.

Operating condition, temperature, and reaction time influenced the reaction pathway of reactants followed to form different product distribution. Further investigation on product distribution leads to identifying the major reactions of each feed. Conversion of olefin feeds of ethylene, propylene, 1-butene, 1-pentene, and 1-hexene for the experimental temperatures and spacetimes are shown in Fig. 5(a) and Fig. 5(b).

Conversion of olefin increased with carbon number among all the feeds with 1-hexene conversion being the highest. The conver-

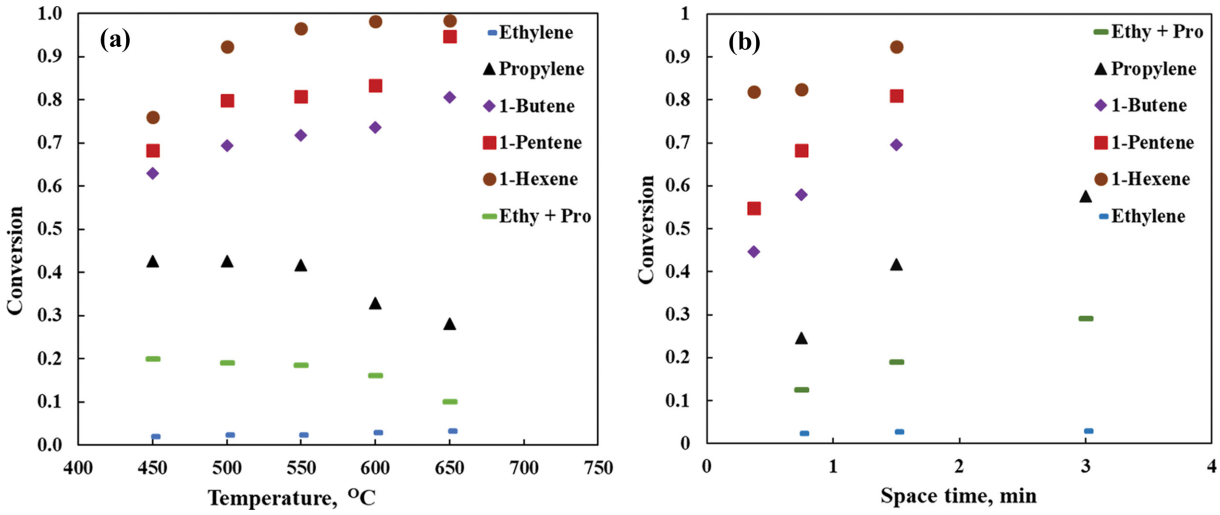

Fig. 5. Effect of temperature for space-time of 1.5 min (a) and effect of space-time at a temperature of 500 °C (b) on conversion.

sion was also increased with increasing temperature and space-time for 1-butene, 1-pentene, and 1-hexene feed. Conversion of 1-hexene increased dramatically up to 500 °C and the rate of increment decreased above that temperature. And for 1-pentene feed conversion was increased in the same fashion as 1-hexene up to 500 °C and remained at lower conversion increment up to 600 °C and a considerable change in conversion from 600-650 °C was observed. 1-Butene conversion also increased with temperature, as [24], though its rate of increment was lower than 1-hexene and 1-pentene. 1-Butene significant change in conversion was noted from 600-650 °C. These differences in the conversion of the feeds over the range of temperature observed due to relative reactivity of feeds based on molecular size, longer molecular size olefin feed require a lower temperature to reach thermodynamic limited equilibrium conversion.

Propylene feed conversion trend behaved differently than the other olefin feeds of having carbon number 4 and above; conversion was increased with contact time but decreased with increasing temperature. A higher reduction in conversion was seen above 550 °C, which indicated propylene feed was more stable at higher temperature or β-scission reaction, the reverse of oligomerization reaction, favored at higher temperature and higher carbon number previously formed oligomers cracked back to propylene. Ethylene conversion, less than 3% in all ranges of temperature and space-time considered, was too low to take its product distribution for further investigation. Therefore, ethylene was taken as non-reactive when contacting the catalyst in the reactor system. Generally, the conversion ranked in order as $C_6>C_5>C_4>C_3>C_2$ and this agrees with the finding of Ying et al. [21].

1. Effect of Temperature on Product Selectivity of Products

The temperature was one of the major parameters which determined the product distribution in the reaction processes. The product distribution of C_2-C_6 olefin feed revealed that, at low temperature, a highly exothermic oligomerization reaction was favored, whereas as the temperature increased, the endothermic β-scission reaction became apparent. Careful qualitative and quantitative analysis on the product distribution of every single feed was used to find a possible reaction pathway of the feed considered in particular and

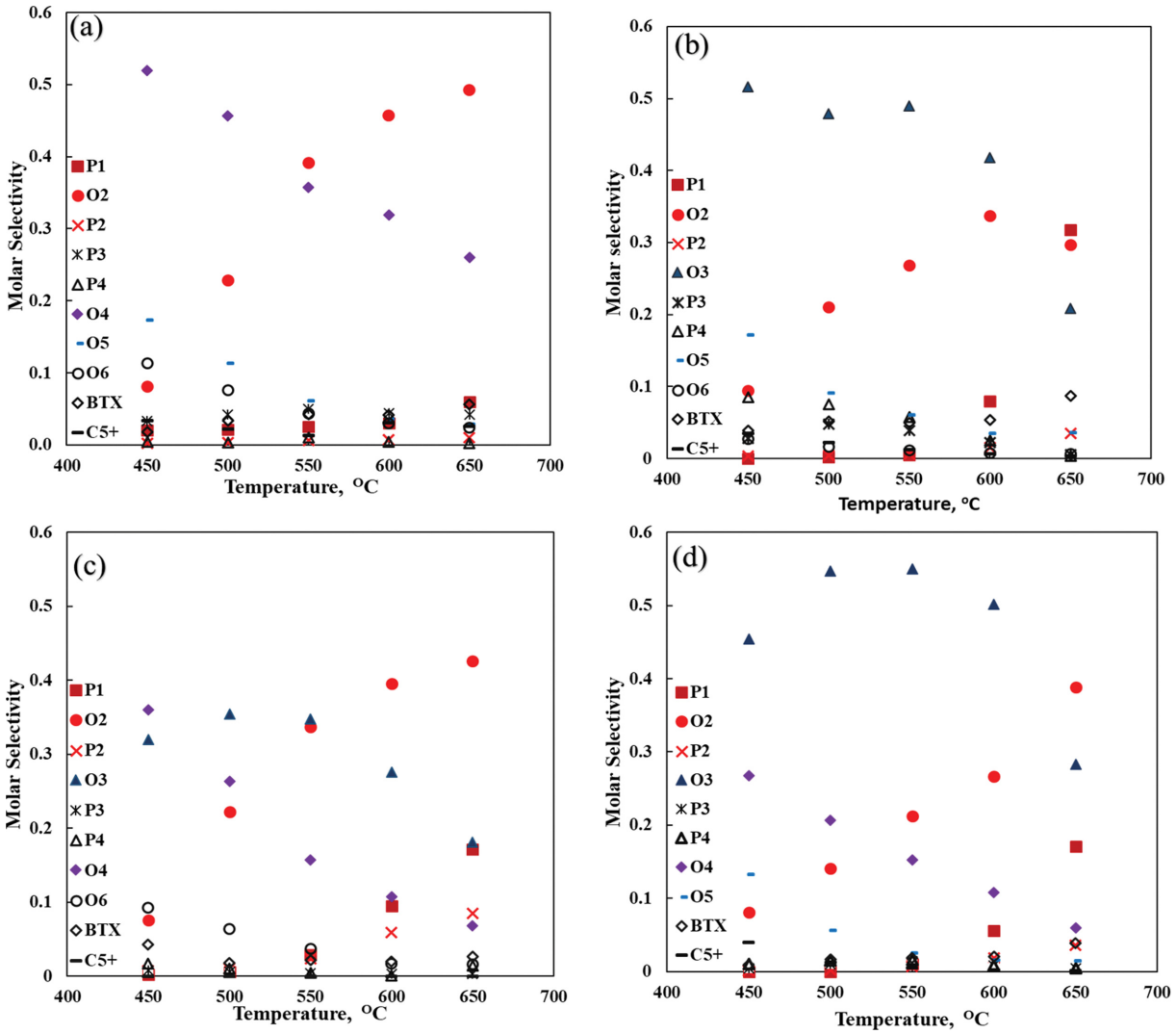

Fig. 6. Temperature influence on product selectivity of olefin feeds (a) propylene, (b) 1-butene, (c) 1-pentene, and (d) 1-hexene feed at WHSV=64 hr^{-1}.

behavior of olefin cracking in general.

1-1. Propylene

Propylene cracking (Fig. 6(a)), resulted in butene and pentene as the primary major products at a lower temperature, 450 °C, followed by hexene and ethylene in order of $C_4>C_5>C_6>C_2$. This indicated that dimerization of propylene (Eq. (3)), formed hexene and hexene again further oligomerized with propylene feed to from C_9 intermediate, Eq. (9), that was cracked to butene and pentene (Eq. (10)). Formed hexene was also cracked in parallel to ethylene and butene (Eq. (2)). Among these reactions, reaction (10) was the fastest. Butene and pentene amount were not equal because part of pentene cracked to ethylene and propylene Eq. (1) and butene was produced also from hexene cracking (Eq. (2)) and from the interaction of formed pentene and propylene feed (Eq. (7)) to give C_8 intermediate that cracked into two butenes Eq. (8). As temperature increased, ethylene production increased more, and primarily formed oligomers are cracked back to lighter olefins (Eqs. (1)-(2)).

1-2. 1-Butene

In 1-butene cracking, initially higher propylene and pentene products were observed at low temperature, which indicated oligomerization reaction took place to give C_8 intermediate before any other further cracking, $C_3>C_5>C_2>C_6$, (Fig. 6(b)). The C_8 oligomer re-cracked to propylene and pentene (Eq. (7)) in parallel with ethylene and hexene (Eq. (6)). Formed hexene further cracked to two moles of propylene (Eq. (3)). Part of pentene was also cracked to ethylene and propylene (Eq. (1)). That was the reason why the amount of propylene was by far higher than other products. Relatively, a lower amount of ethylene formation at the lower temperature indicated that direct cracking of butene to 2 moles of ethylene was difficult, because this reaction required higher energy than other possible reactions, as discussed in other works [12,21]. As mentioned earlier in propylene feed, in 1-butene cracking, higher temperature favored a higher amount of ethylene because primarily formed pentene and other higher olefins cracked back to ethylene and propylene (Eqs. (1)-(4)).

1-3. 1-Pentene

Unlike propylene and 1-butene cracking, the case in 1-pentene cracking follows a different route. From the product distribution, as shown in Fig. 6(c), both β-scission cracking and oligomerization reactions appear in parallel at a lower temperature, though oligomerization reaction is more dominant (Eqs. (1), and (11)-(13)). From the formation of olefin products in order $C_4>C_3>C_6>C_2$, it can be understood that butene came from oligomerization reaction and propylene came either from a direct cracking of the feed as a primary product or as a tertiary product from the re-cracking of hexene dimer. Hexene was expected to be formed from oligomerization reaction at equal amount with butene (Eq. (12)), but due to its high activity, it converted to other products immediately after its formation and formed butene and ethylene as Eq. (2) or two moles of propylene (Eq. (3)).

1-4. 1-Hexene

As shown in Fig. 6(d), 1-hexene cracking follows direct cracking into two propylene (Eq. (3)) or ethylene and butene (Eq. (2)). Olefin product distribution with carbon number, $C_3>C_4>C_5>C_2$, appeared first and butene and ethylene were not equimolar, butene amount was much higher. The difference in the amount of ethylene and butene is explained in line with the formation of pentene. Pentene was not obtained from a direct cracking of 1-hexene. The two major products in propylene cracking at low temperature, butene, and pentene, also appeared here. Therefore, it is evident that the formed propylene reacted further with the feed 1-hexene to form C_9 intermediate (Eq. (9)), that cracked to butene and pentene (Eq. (10)) as previously discussed in propylene cracking. Primary β-scission products of 1-hexene, propylene and ethylene, may also have reacted to form heterodimer C_5 olefin which further reduced ethylene amount at a lower temperature (Eq. (1)). As temperature increased, ethylene amount increased in the same fashion as it did in other feeds. This lower amount of ethylene at a lower temperature in all feeds agrees with other previous works, too [4,18,19,21].

1-5. Identified Reactions

The following thirteen reversible reactions are identified as major reactions in olefin cracking based on the product distribution from each feed. These reactions were also used for kinetic parameter estimation. For convenience, all forward reactions are β-scission (direct cracking) reactions, whereas the backward reactions are oligomerization (homo and heterodimerization) reactions.

$$C_5H_{10} \rightleftharpoons C_2H_4+C_3H_6 \quad (1)$$

$$C_6H_{12} \rightleftharpoons C_2H_4+C_4H_8 \quad (2)$$

$$C_6H_{12} \rightleftharpoons 2C_3H_6 \quad (3)$$

$$C_7H_{14} \rightleftharpoons C_2H_4+C_5H_{10} \quad (4)$$

$$C_7H_{14} \rightleftharpoons C_3H_6+C_4H_8 \quad (5)$$

$$C_8H_{16} \rightleftharpoons C_2H_4+C_6H_{12} \quad (6)$$

$$C_8H_{16} \rightleftharpoons C_3H_6+C_5H_{10} \quad (7)$$

$$C_8H_{16} \rightleftharpoons 2C_4H_8 \quad (8)$$

$$C_9H_{18} \rightleftharpoons C_3H_6+C_6H_{12} \quad (9)$$

$$C_9H_{18} \rightleftharpoons C_4H_8+C_5H_{10} \quad (10)$$

$$C_{10}H_{20} \rightleftharpoons C_3H_6+C_7H_{14} \quad (11)$$

$$C_{10}H_{20} \rightleftharpoons C_4H_8+C_6H_{12} \quad (12)$$

$$C_{10}H_{20} \rightleftharpoons 2C_5H_{10} \quad (13)$$

Further analysis in all C_2-C_6 feeds showed, as temperature increased, a considerable amount of other products like BTX and paraffin were produced. A significantly high amount of methane was also obtained at 650 °C. This presence of paraffin and BTX at higher temperatures can be explained by aromatization reaction. For aromatization reaction, prior cyclization of C_6-C_8 olefins occurs to form C_6-C_8 naphthenes as an intermediate, and then hydride transfer reaction between the naphthenes and C_2-C_4 light olefins gives C_6-C_8 aromatics (benzene, toluene, and xylene (BTX)) and corresponding light paraffin (C_2-C_4) (Eq. (14)), the general form of aromatization reaction [23,25].

$$(N_6-N_8)+3(C_2\text{-}C_4)\ \text{olefins} \rightarrow \text{BTX}+3(C_2\text{-}C_4)\ \text{paraffins} \quad (14)$$

Once light alkanes are formed from aromatization reaction (Eq.

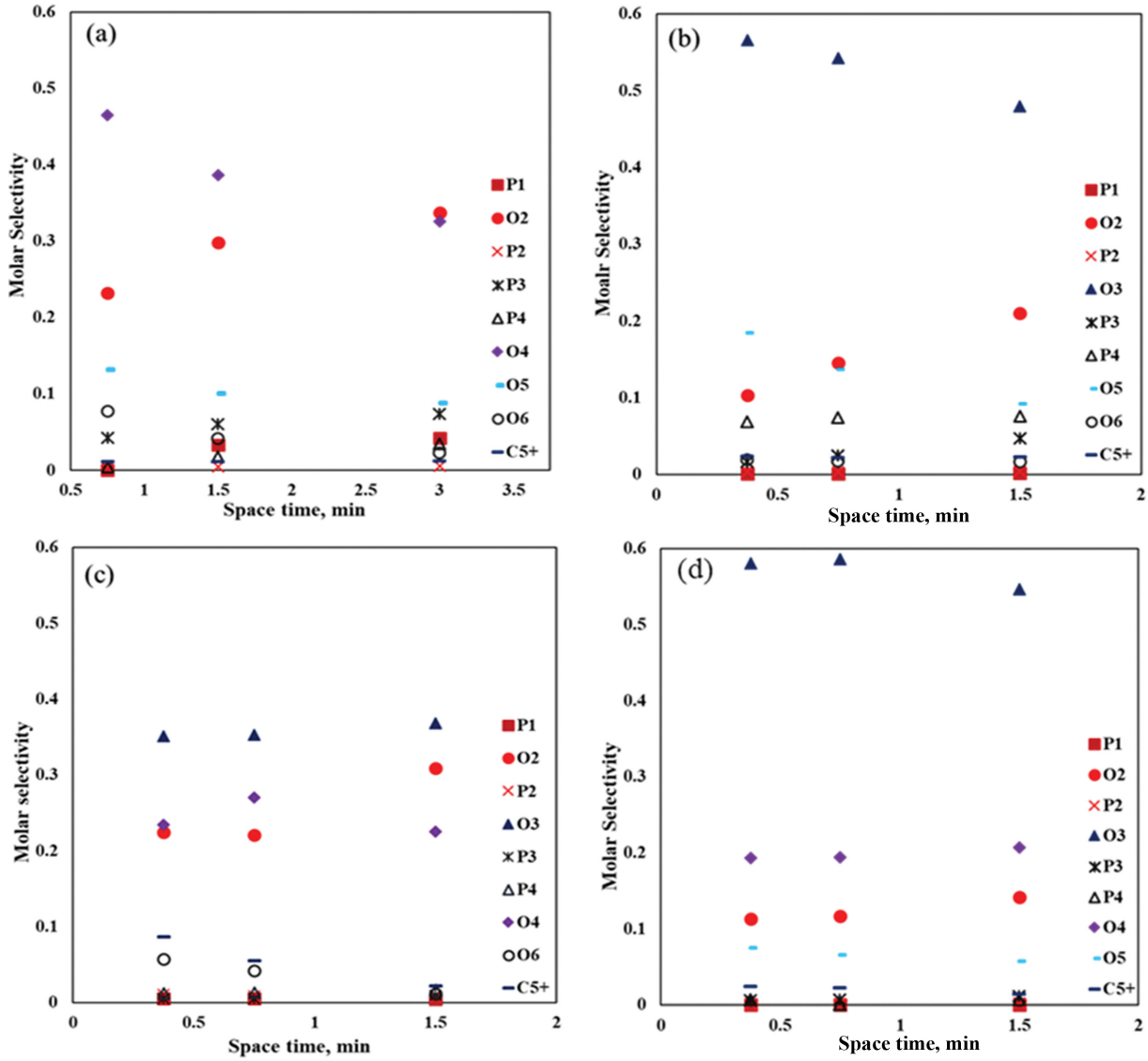

Fig. 7. Space-time influence on product selectivity of products for olefin feed (a) propylene, (b) 1-butene, (c) 1-pentene, and (d) 1-hexene feed at 500 °C.

(14)), paraffin cracking on ZSM-5 catalyst indicates ethane remains stable and part of butane and propane will undergo protolytic cracking to form methane and corresponding olefins. Methane was the major product of n-butane cracking [7,8]. Therefore, propane and butane formed from aromatization reaction were the sources of methane observed at elevated temperatures (Eqs. (15) and (16)). The model excluded aromatization reactions to reduce complexity.

$$C_4H_{10} \rightarrow CH_4 + C_3H_6 \quad (15)$$

$$C_3H_8 \rightarrow CH_4 + C_2H_4 \quad (16)$$

Experimental quantification of higher carbon olefins was difficult because they are highly active to be formed and changed to other products in a short contact time. Identification of reactions was solely based on the final product distribution for each feed. Generally, ethylene selectivity increases with temperature because higher olefins cracked to smaller carbon olefins at higher temperature, whereas propylene selectivity increased initially up to 550 °C and decreased at high temperature.

2. Effect of Space-time on Product Selectivity

Space-time also plays an important role in the selectivity of products as temperature (Fig. 7). Short contact time promoted oligomerization reactions as the lower temperature did and, as a result, higher molecular products were produced. As time increases, the pre-formed oligomer cracked back to lighter olefin products.

The product distribution of propylene cracking in Fig. 7(a) indicates formation of $C_4 > C_2 > C_5 > C_6$ was a result of the dimerization reaction of the feed (Eq. (3)) to form hexene, and hexene was reactive to cracking further into ethylene and butene (Eq. (2)). Again, as it was discussed earlier at low-temperature, pentene and butene formed from hexene and propylene dimer C_9 (Eqs. (9) and (10)) at short contact time. As contact time increased, the amount of higher carbon number olefins decreased and that of ethylene increased as a result of re-cracking of these reactive oligomers.

Propylene and pentene were the primary products of 1-butene cracking at the short contact time (Fig. 7(b)). This was because 1-butene oligomerized to C_8 (Eq. (8)) intermediate before cracking to propylene and pentene (Eq. (7)). As contact time increased, both propylene and pentene amounts decreased to compensate for the increased amount of ethylene (Eq. (1)); this result agreed with [4,19,21].

With a little different fashion from the other feeds, short contact time product distribution for 1-pentene feed also promoted higher olefin formation like butene accompanied with lighter olefins of propylene and ethylene (Fig. 7(c)). This was because at short contact time both dimerization (Eq. (13)), re-cracking of the dimer (Eqs. (11) and (12)), and direct cracking of 1-pentene (Eq. (1)) took place in parallel. As the contact time increased direct cracking of pentene into ethylene and propylene reaction became dominant and, as a result, ethylene and propylene amount became close to equimolar.

For 1-hexene cracking, a higher amount of propylene followed by butene and ethylene (Fig. 7(d)), was a direct cracking reaction of 1-hexene into two propylene in parallel with into ethylene and butene (Eqs. (2) and (3)). Further qualitative analysis is similar to the previous discussion on the influence of temperature.

ETHYLENE AND PROPYLENE MIX FEED

Ethylene feed showed lower activity and was considered non-reactive when fed as a single feed. For ethylene and propylene mix feed, half of the propylene was substituted with an equal mole of ethylene. If ethylene was non-reactive in the mixture feed, as it was when used as a single feed, the amount of pentene produced in the ethylene-propylene mix should have been half of the amount produced from propylene feed alone. The result indicated the amount of pentene produced from the ethylene-propylene mixture was much higher than the expected amount of considering ethylene as non-reactive. The amount of pentene from the mixture feed increased with contact time and became equal at higher contact time. This indicated that at this contact time half of the pentene came from direct interaction of ethylene and propylene, which provided evidence that ethylene and propylene interacted as mentioned in the reverse reaction of Eq. (1). This interaction of ethylene and propylene agreed with previous works of Liu et al. [13].

Finally, in all feeds, it was found out ethylene prefers higher temperature and longer contact time, but propylene prefers a relatively lower temperature and shorter contact time. That is one of the advantages of catalytic cracking to control the product distribution by knowing the optimum working condition for the desired product needed.

KINETIC MODEL

1. Equation for Parameter Estimation

The experimental data obtained in the temperature range of 450-550 °C was used for parameter estimation, and the fitting of each feed for 450 and 550 °C temperature is shown in Fig. 8 and Fig. 9 where points represent experimental data and lines for predicted calculated values. For the experiments conducted in the fixed-bed microreactor, a plug flow and isothermal condition with no pressure drop were assumed.

The predictive response ($\hat{y}_1$) was calculated from the following continuity equation:

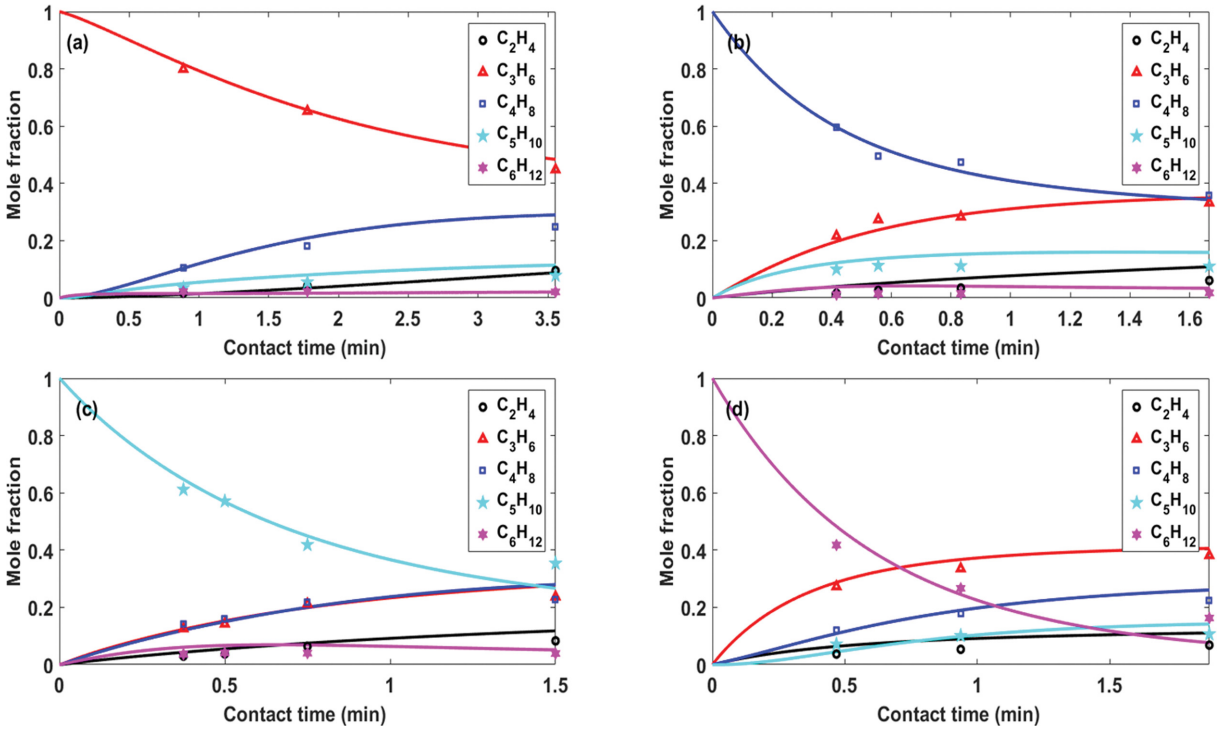

Fig. 8. Fitting of experimental result with model prediction (a) propylene, (b) 1-butene, (c) 1-pentene and (d) 1-hexene feed at 450 °C.

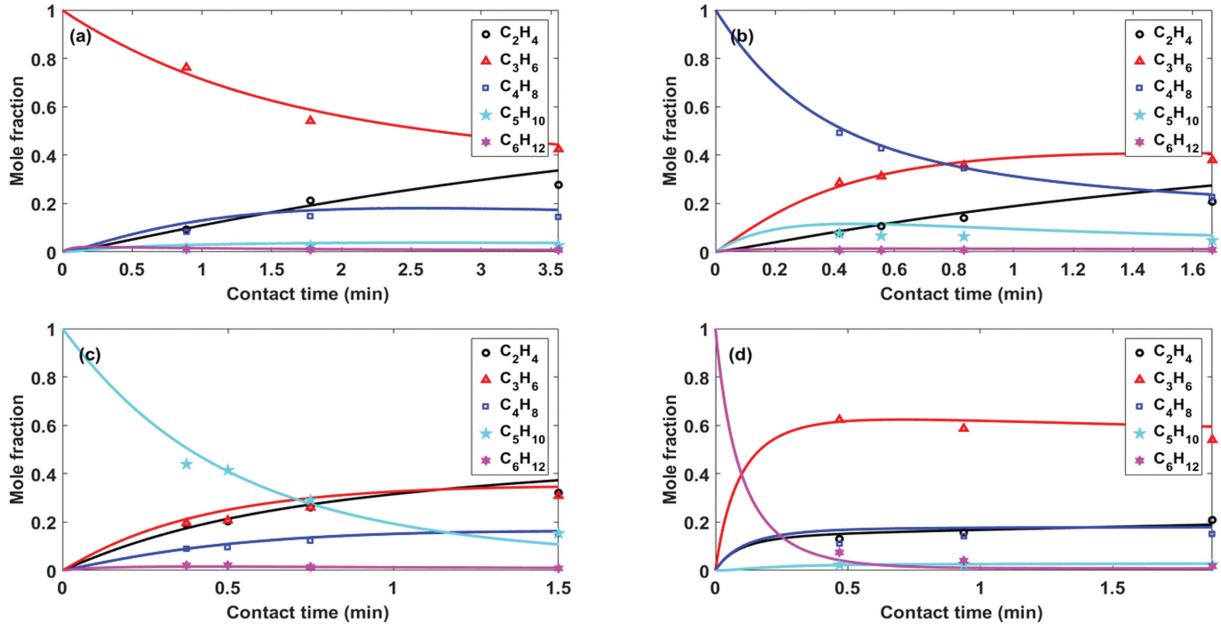

Fig. 9. Fitting of experimental result with model prediction (a) propylene, (b) 1-butene, (c) 1-pentene, and (d) 1-hexene feed at 550 °C.

$$\frac{d(\hat{y}_i)}{d\left(\frac{W}{F_{0,\,feed}}\right)} = \Sigma_j \alpha_{j,\,i} r_j \tag{17}$$

$$P_i = P_t \hat{X}_i \tag{18}$$

$$\hat{X}_i = \frac{\hat{y}_i}{\Sigma \hat{y}_i + y_d} \tag{19}$$

where $\hat{y}_1$ is the molar yield of species i, mole-formed per initial mole flow rate including dilution; W is the amount of catalyst in g; $F_{0,feed}$ is feeding rate hydrocarbon in $gmin^{-1}$; $\alpha_{j,i}$ is the stoichiometric coefficient of i-species of j^{th} reaction; and r_j is reaction rate of j^{th} reaction. P_t is total pressure which was kept in 1 atm; $\hat{X}_1$ is predicted mole fraction of i-species; y_d is dilution ratio in the initial state. The values of k_{j0} and $E_{app,j}$ were estimated simultaneously with genetic algorithms for global search and interior-point method for local search using MATLAB. Parameter estimation was based on the minimization of residual objective function OF given by Eq. (20).

$$OF = \Sigma_{k=1}^{N_T} \Sigma_{l=1}^{N_{exp}} \Sigma_{i=1}^{N_i} (X_{i,\,l,\,k} - \hat{X}_{i,\,l,\,k})^2 \tag{20}$$

$X_{i,l,k}$ are $\hat{X}_{i,\,l,\,k}$ mole fractions of experimental data and model-predicted data; N_T, N_{exp}, N_i are the number of temperature points, experimental points, and species respectively. Subscripts i, l, k represents i-species, l-experiment point, and k-number of temperatures, respectively.

2. Model Results and Discussion

Experimental results showed ethylene does not react when fed as a single feed, but reacts when co-fed as a mixture with propylene. This indicate that the adsorption rate of ethylene was slower than its surface reaction. Therefore, in the case of ethylene bimolecular reaction, the adsorption rate of ethylene was taken as the rate-determining step and, as a result, backward reactions r_1, r_2, r_4, and r_6 were found to have almost the same kinetic parameters.

Since adsorption energy for olefins has a negative value [21], the apparent activation energy, which is the sum of adsorption energy and actual activation energy, can be positive for activation energy value higher than the adsorption energy and negative for activation energy value less than that of the adsorption energy. Depending on the reaction step, either two adjacent sites or a single site might be involved during the oligomerization reaction. The apparent activation energy is mostly negative for adjacent site oligomerization and, depending on the value, might be negative or positive for single-site oligomerization so that reactions 3, 5, 7, and 8 might follow a single site reaction mechanism.

As expected, for identified reactions, the activation energy of the backward exothermic oligomerization reaction was much smaller than that of the forward endothermic β-scission reaction. This indicates that the enthalpy from the adsorption reaction contributed to the lower apparent activation energy demand of the oligomerization reaction than the β-scission reaction.

For calculated kinetic parameters of identified reactions shown in Table 2, $k_{o,f}$ and $k_{o,b}$ were reaction rate constants calculated at a reference temperature of 450 °C, and $E_{a,f}$ and $E_{a,b}$ were the apparent activation energy for forward and backward reactions, respectively.

In previous works, the apparent activation energy was found negative for bimolecular reaction and positive for the β-scission reaction [4,21]. In this work, it was also found positive apparent activation for β-scission reactions, but both negative and positive apparent activation energies were observed among bimolecular dimerization reactions. This might happen due to the number of sites involved for adsorption in bimolecular reactions.

Thus, all reactions can fall into either of the two types of known reaction mechanisms. Reactions 3, 5, 7, 8, and 10 with positive apparent activation energy followed the Eley-Rideal reaction mech-

Table 2. Estimated kinetic parameters

No.	Reactions	$k_{o,f}$	$k_{o,b}$	$E_{a,f}$	$E_{a,b}$
		$(L\cdot mol^{-1})^n\cdot g_{feed}\cdot g_{cat}^{-1}\ min^{-1}$		$kJmol^{-1}$	
1.	$C_5H_{10}\rightleftharpoons C_2H_4+C_3H_6$	1.85E+01	1.16E+04	109.74	−60.00
2.	$C_6H_{12}\rightleftharpoons C_2H_4+C_4H_8$	1.60E+02	1.16E+04	109.74	−60.00
3.	$C_6H_{12}\rightleftharpoons 2C_3H_6$	4.35E+02	1.03E+04	99.82	69.73
4.	$C_7H_{14}\rightleftharpoons C_2H_4+C_5H_{10}$	8.76E+03	1.16E+04	109.72	−60.00
5.	$C_7H_{14}\rightleftharpoons C_3H_6+C_4H_8$	1.71E+04	1.39E+04	94.62	60.44
6.	$C_8H_{16}\rightleftharpoons C_2H_4+C_6H_{12}$	2.22E+04	1.16E+04	95.01	−60.00
7.	$C_8H_{16}\rightleftharpoons C_3H_6+C_5H_{10}$	1.11E+05	1.60E+05	94.61	60.42
8.	$C_8H_{16}\rightleftharpoons 2C_4H_8$	1.11E+05	9.56E+04	0.87	0.52
9.	$C_9H_{18}\rightleftharpoons C_3H_6+C_6H_{12}$	8.40E+03	9.70E+05	94.60	46.13
10.	$C_9H_{18}\rightleftharpoons C_4H_8+C_5H_{10}$	8.60E+03	2.07E+05	0.01	−15.52
11.	$C_{10}H_{20}\rightleftharpoons C_3H_6+C_7H_{14}$	1.53E+05	7.76E+07	94.54	46.10
12.	$C_{10}H_{20}\rightleftharpoons C_4H_8+C_6H_{10}$	1.53E+05	5.19E+02	94.54	94.50
13.	$C_{10}H_{20}\rightleftharpoons 2C_5H_{10}$	1.61E+05	6.40E+04	6.00	−24.43

anism on which two molecules adsorbed on the surface before reaction. And all other reactions showed negative apparent activation energy following the Langmuir-Hinshelwood mechanism, a mechanism that one molecule adsorbed on the surface and the other molecule reacted with the molecule previously adsorbed on the surface without using another active site of the catalyst.

Calculated values of apparent activation energy varied from −60.0-109.74 $kJmol^{-1}$. In all cases, the endothermic forward reaction has less apparent activation than the backward exothermic reactions. This agrees with experimental results of lower temperature favored oligomerization reaction and higher temperature favored β-scission reactions. Comparison of kinetic parameters with other works was done. But a little deviation was observed because the catalyst used for this work was more acidic than in previously reported works and the reactions considered for the model were also a little different. Kinetic coefficient value varies 1.85E+01 $(L\cdot mol^{-1})\cdot g_{feed}\cdot g_{cat}^{-1}\ min^{-1}$ for β-scission reaction of pentene in to ethylene and propylene to 7.76E+07 $(L\cdot mol^{-1})^2\cdot g_{feed}\cdot g_{cat}^{-1}\ min^{-1}$ dimerization of C_3 and C_7 to form higher carbon number C_{10} intermediate Eq. (11).

Calculated apparent activation energy and kinetic constant showed the reactivity order of parallel reactions from higher carbon number olefins. Propylene, 1-butene, and 1-pentene feed formed dimers before further cracking. Thus, C_6 intermediate or feed had two alternative routes either to be cracked into two moles of propylene or ethylene and butene. The former reaction was preferred more due to less activation energy and higher kinetic constant than the latter. This agreed well with high propylene product observation from the 1-hexene feed. C_7 intermediate which had two routes into ethylene and pentene or propylene and butene. Here propylene and butene route was preferred due to less activation energy and higher kinetic constant. When the C_8 intermediate was observed there were three possible routes: C_8 can be cracked into C_2 and C_6, C_3 and C_5, or into two C_4 molecules. The same comparison on apparent activation energy and kinetic constant revealed C_8 into two C_4 molecules was the most preferred route followed by C_8 into C_3 and C_5 and C_8 into C_2 and C_6 was less preferred. For C_9 intermediate C_9 into C_4 and C_5 route was more preferred than C_9 into C_3 and C_6. And for C_{10} intermediate C_{10} into two C_5 was followed by C_{10} into C_4 and C_6 and C_{10} into C_3 and C_7.

Generally, from the analysis of Table 2, it is evident that even carbon number olefins, obviously except butene, preferred symmetrical cracking off into two identical molecules followed by the propylene route. And odd carbon intermediate or feed preferred propylene route. That indicated why ethylene production needed a higher temperature than propylene, as seen in the experimental product distribution.

The kinetic model predicted results were compared with experimental results of different temperatures for C_2-C_6 feed for each component in the product distribution (Fig. 8 and Fig. 9). It was found that the kinetic model predicted the experimental result well with some deviation. Some of the predicted amounts were higher or lower than the actual experimental results, which indicated that some reactions needed to be removed or added to balance formation and consumption of species for a better fitting. As the temperature increased, the deviation between model and experimental values became more evident due to higher conversion and involvement of many species for parallel reactions.

Parity plot of all feeds (Fig. 10) showed model values agree with

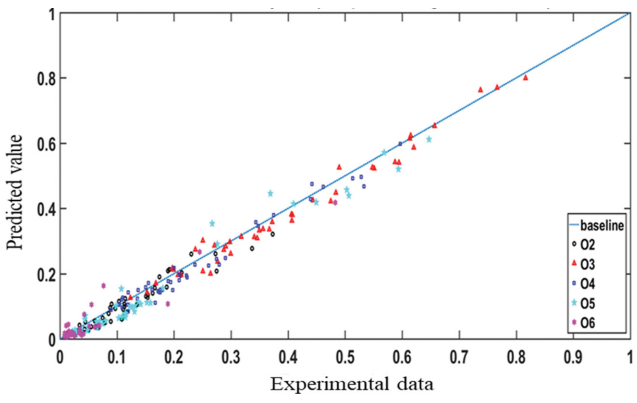

Fig. 10. Parity plot for all olefin feeds in the range of 450-550 °C.

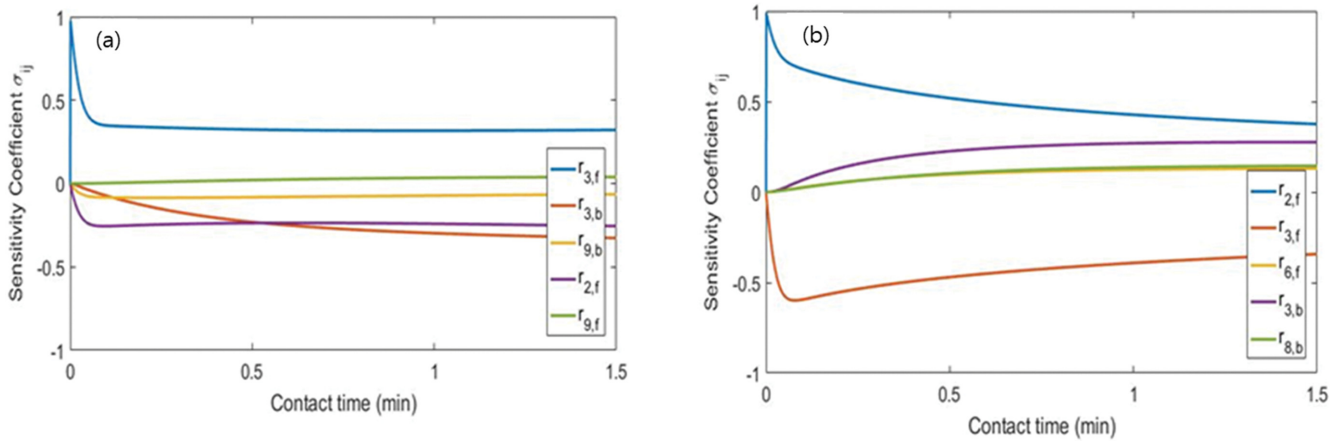

Fig. 11. Sensitivity analysis of 1-hexene feed for (a) ethylene yield (b) propylene yield.

experimental values except for a few points. These deviations especially came for 1-hexene because hexene was highly reactive compared to other olefins considered as a feed and its high conversion might need better accuracy of product detection and quantification. Most predicted values of the model, if not all, fit well with experimental results with an R^2 value of 0.8812 for ethylene, 0.9718 for propylene, 0.9592 for butene, 0.9563 for pentene, and 0.8735 for hexene. Ethylene and hexene showed lower R^2 values and for ethylene, this might arise from either assumption of ethylene non-reactive incurred error to the computation or from experimental error, and for hexene, the deviation might be from higher hexene reactivity to undergo parallel side reactions.

Main production routes of ethylene and propylene were identified from each feed using the sensitivity analysis method. It was observed that sensitivity was higher at short contact time for dominant reactions, but the longer the contact time the less sensitivity among reactions. In most of the cases, propylene and ethylene production routes competed as observed also in product distributions. Sensitivity of reactions for 1-hexene feed showed the two competent reactions $C_6H_{12} \rightarrow 2C_3H_6$ affect propylene yield positively and ethylene negatively. And the other reaction $C_6H_{12} \rightarrow C_2H_4+C_4H_8$ affects propylene yield negatively and vice versa for ethylene (Fig. 11). Details of sensitivity analysis for other feeds are explained in supporting information.

CONCLUSIONS

In a catalytic olefin olefin conversion over ZSM-5 catalyst short-chain olefins oligomerize before cracking and the longer chain olefins directly cracked to light olefins. Oligomerization reaction is favored at lower temperatures but at high-temperature β-scission reaction becomes dominant. The apparent activation energy of the reaction path, which is the result of adsorption and surface reaction, was both negative and positive for exothermic oligomerization reaction and positive for endothermic β-scission reaction.

Ethylene was not active when fed to reactor alone, and from this it was assumed ethylene adsorption was too slow and taken as the slowest step, rate-determining step of the system, but ethylene behaved differently and participated in the reaction when it was co-fed as a mixture with propylene. A higher amount of pentene product in the mixture feed of propylene and ethylene than propylene feed alone showed these two important hydrocarbons undergo dimerization reaction.

Main production routes for ethylene and propylene yield have been identified using sensitivity analysis. Propylene and 1-butene olefin feed affect the yield of ethylene and propylene positively if they make dimer first. Upon the re-cracking of the dimer, both ethylene and propylene routes were competent reactions. Reactions positively affecting ethylene production are seen affecting propylene yield negatively.

Propylene was highly selective at lower temperature and short contact time but ethylene preferred higher temperature and longer contact time. C_2-C_6 feed shows a dominant propylene product below 550 °C, which was typically from catalytic performance, but above 600 °C ethylene took dominancy from significant thermal cracking contribution.

The performed experimental results on C_2-C_6 for a wide range of temperatures fit well with the developed kinetic model. This model can predict kinetic parameters in a good manner so that it can be used to determine kinetic behavior in processes involving olefins as feed, intermediate, or products.

ACKNOWLEDGEMENTS

The authors are grateful to the National Research Council of Science & Technology (NST) of Korea (the R&D Convergence Program, Center for Convergent Chemical Process (CCP), CRC-14-1-KRICT) and the Korea Research Institute of Chemical Technology (KK2012-00) for financial support.

AUTHOR CONTRIBUTIONS

Ashenafi Hailu Berta and H. D. Hwang contributed equally to this work.

NOTES

The authors declare no competing financial interest.

SUPPORTING INFORMATION

Additional information as noted in the text. This information is available via the Internet at http://www.springer.com/chemistry/journal/11814.

REFERENCES

1. S. Sadrameli, *Fuel*, **173**, 285 (2016).
2. S. Sadrameli, *Fuel*, **140**, 102 (2015).
3. S. Standl and O. Hinrichsen, *Catalysts*, **8**, 626 (2018).
4. F. Warnecke, L. Lin, S. P. Haag and H. R. Freund, *Ind. Eng. Chem. Res.*, **59**, 12696 (2020).
5. S. Standl, T. Kuhlewind, M. Tonigold and O. Hinrichsen, *Ind. Eng. Chem. Res.*, **58**, 18107 (2019).
6. Y.-H. Guo, M. Pu, B.-H. Chen and F. Cao, *Appl. Catal. A-Gen.*, **455**, 65 (2013).
7. H. Krannila, W. Haag and B. Gates, *J. Catal.*, **135**, 115 (1992).
8. T. F. Narbeshuber, H. Vinek and J. A. Lercher, *J. Catal.*, **157**, 388 (1995).
9. A. Coelho, G. Caeiro, M. Lemos, F. Lemos and F. R. Ribeiro, *Fuel*, **111**, 449 (2013).
10. E. Epelde, A. S. T. Aguayo, M. Olazar, J. Bilbao and A. G. Gayubo, *Ind. Eng. Chem. Res.*, **53**, 10599 (2014).
11. E. Epelde, A. G. Gayubo, M. Olazar, J. Bilbao and A. T. Aguayo, *Chem. Eng. J.*, **251**, 80 (2014).
12. C.-J. Chen, S. Rangarajan, I. M. Hill and A. Bhan, *Acs Catal.*, **4**, 2319 (2014).
13. D. Liu, W. C. Choi, N. Y. Kang, Y. J. Lee, H. S. Park, C.-H. Shin and Y.-K. Park, *Catal. Today*, **226**, 52 (2014).
14. D. B. Lukyanov, N. S. Gnep and M. R. Guisnet, *Ind. Eng. Chem. Res.*, **33**, 223 (1994).
15. S. Tabak, F. Krambeck and W. Garwood, *AIChE J.*, **32**, 1526 (1986).
16. J. H. Lee, S. Kang, Y. Kim and S. Park, *Ind. Eng. Chem. Res.*, **50**, 4264 (2011).
17. J. Abbot and B. Wojciechowski, *Can. J. Chem. Eng.*, **63**, 462 (1985).
18. J. Buchanan, J. Santiesteban and W. Haag, *J. Catal.*, **158**, 279 (1996).
19. X. Huang, D. Aihemaitijiang and W.-D. Xiao, *Chem. Eng. J.*, **280**, 222 (2015).
20. H. Voge, G. Good and B. Greensfelder, *Ind. Eng. Chem.*, **38**, 1033 (1946).
21. L. Ying, J. Zhu, Y. Cheng, L. Wang and X. Li, *J. Ind. Eng. Chem.*, **33**, 80 (2016).
22. J. Li, T. Li, H. Ma, Q. Sun, C. Li, W. Ying and D. Fang, *Chem. Eng. J.*, **346**, 397 (2018).
23. M. Guisnet, N. Gnep, D. Aittaleb and Y. Doyemet, *Appl. Catal. A-Gen.*, **87**, 255 (1992).
24. P. Borges, R. R. Pinto, M. Lemos, F. Lemos, J. Védrine, E. Derouane and F. R. Ribeiro, *Appl. Catal. A-Gen.*, **324**, 20 (2007).
25. Y. Song, X. Zhu and L. Xu, *Catal. Commun.*, **7**, 218 (2006).

Supporting Information

Reaction mechanism and kinetic modeling of olefin conversion over phosphorus modified ZSM-5 catalyst

Ashenafi Hailu Berta*,,‡, Ho Dong Hwang*,**,‡, Hagos Birhane Asfha*,**, Na Young Kang*, Kiwoong Kim*,†, and Yong-Ki Park*,†**

*Center for Convergent Chemical Process, Korea Research Institute of Chemical Technology (KRICT), Gajeong-ro 141, Yuseong-gu, Daejeon 34114, Korea
**Advanced Materials and Chemical Engineering, University of Science and Technology (UST), Gajeong-ro 217, Yuseong-gu, Daejeon 34113, Korea
(*Received 14 October 2021 • Revised 17 November 2021 • Accepted 17 November 2021*)

1. Ethylene Propylene Mixed Feed

For ethylene and propylene mix half of propylene was substituted with ethylene and result showed, Fig. S1, that pentene amount form the mixture feed was not half of its value indicating ethylene was reacted with propylene to give pentene as an agreement with other work [1].

2. Kinetic Parameter Estimation

Reaction rate was simplified based on the Langmuir Hinshelwood Hougen Watson (LHHW) approach.

$$r_j = \frac{k_j' \Pi_{\alpha_{j,i}<0} \left(K_i \frac{P_i}{RT}\right)^{-\alpha_{j,i}}}{1+\Sigma K_i P_i} \tag{1}$$

Where k_j' is surface reaction rate constant for j^{th} reaction; P_i is partial pressure for i-species; and K_i is adsorption equilibrium constant for i-species; if $\Sigma K_i P_i$ is smaller than 1, Eq. (1) could be simplified into Eq. (2)

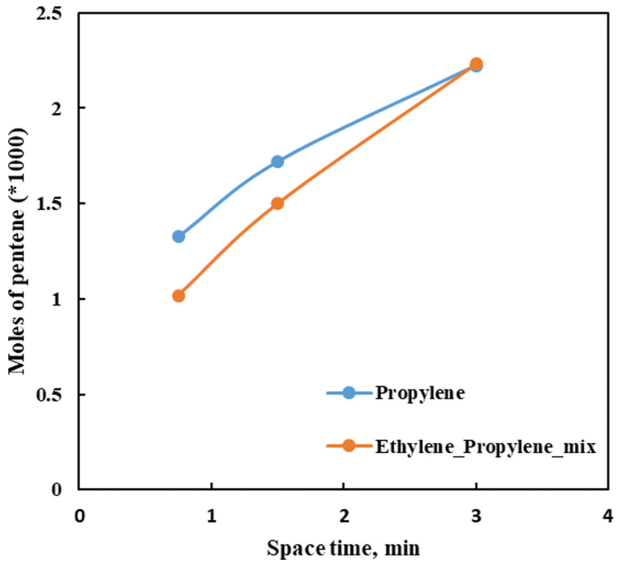

Fig. S1. Pentene product comparison for propylene and mixture of propylene and ethylene feed at 500 °C.

$$r_j \approx \Pi K_i^{-\alpha_{j,i}} k_j' \Pi_{\alpha_{i,j}<0} \left(\frac{P_i}{RT}\right)^{-\alpha_{j,i}} \tag{2}$$

The dependence of temperature on the equilibrium and surface kinetic constant were represented by using Arrhenius and Van't hoff equations respectively and it was combined into apparent activation energy Eqs. (3)-(7).

$$K_i = K_{i,0} \exp\left(\frac{-\Delta H_{ads,i}}{R}\left(\frac{1}{T}-\frac{1}{T_{ref}}\right)\right) \tag{3}$$

$$k_j' = k_{j,0}' \exp\left(\frac{-E_{a,j}}{R}\left(\frac{1}{T}-\frac{1}{T_{ref}}\right)\right) \tag{4}$$

$$E_{app,j} = E_{a,j} - \Sigma \alpha_{j,i} \Delta H_{ads,i,j} \tag{5}$$

$$k_{j,0} = k_j' \Pi K_{i,j} \tag{6}$$

$$k_j = k_{j,0} \exp\left(\frac{-E_{app,j}}{R}\left(\frac{1}{T}-\frac{1}{T_{ref}}\right)\right) \tag{7}$$

$K_{j,0}$, $k_{j,0}'$, $k_{j,0}$ are adsorption equilibrium, surface kinetic rate and apparent kinetic rate constant for j^{th} reaction at reference temperature (723 K) respectively; k_j is apparent kinetic rate constant; E_a, $E_{a,app}$ are activation energy and apparent activation energy in kJ/mol; R is gas constant; T is temperature in K and T_{ref} is reference temperature.

3. Sensitivity Analysis

Main production routes of ethylene and propylene were identified from each feed using sensitivity analysis method. Experimental results showed that the product composition changed quickly with time. As reaction rate depend on product composition, the reaction rate was also changed quickly. The sensitivity analysis was carried out for ethylene and propylene yield over reaction contact time at 500 °C. Among the total 26 forward and backward reactions, the top five reactions highly sensitive for each feed for the desired product to be maximized identified. Sensitivity coefficient σ_{ij} computed as:

$$\sigma_{ij} = \frac{k_j}{\hat{X}_i} \frac{\partial \hat{X}_i}{\partial k_j} \tag{8}$$

Where $\hat{X}_i$ and k_j are mole fraction of desired product, ethylene

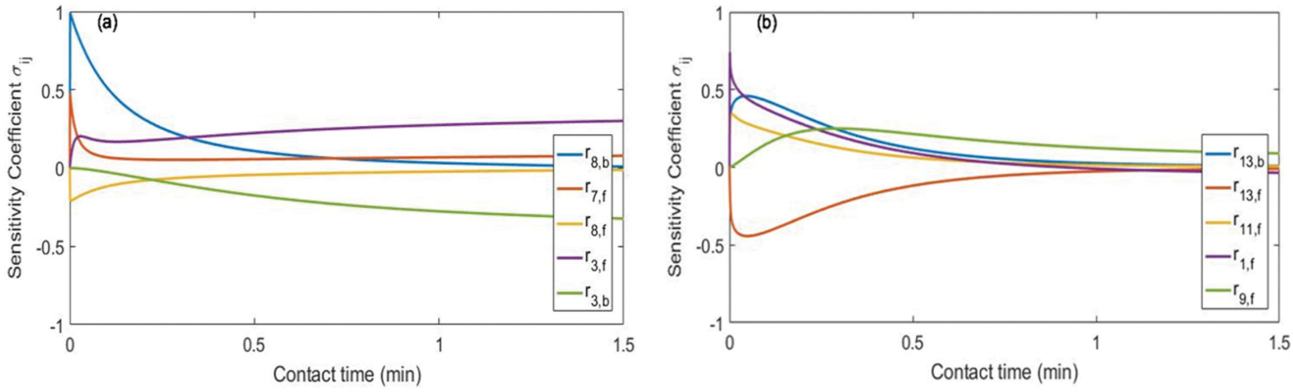

Fig. S2. Sensitivity analysis on propylene yield from different feeds; (a) 1-butene, and (b) 1-pentene.

Table S1. Sensitivity analysis summary

Product considered	Feed type	Major sensitive reactions	Effect
Ethylene	Propylene	$2C_3H_6 \rightarrow C_6H_{12}$	Positive
		$C_6H_{12} \rightarrow C_2H_4 + C_4H_8$	Positive
		$C_6H_{12} \rightarrow 2C_3H_6$	Negative
	1-Butene	$2C_4H_8 \rightarrow C_8H_{16}$	Positive
		$C_8H_{16} \rightarrow C_2H_4 + C_6H_{12}$	Positive
		$C_8H_{16} \rightarrow C_3H_6 + C_5H_{10}$	Negative
	1-Pentene	$C_5H_{10} \rightarrow C_2H_4 + C_3H_6$	Positive
		$C_8H_{16} \rightarrow C_3H_6 + C_5H_{10}$	Negative
Propylene	1-Butene	$2C_4H_8 \rightarrow C_8H_{16}$	Positive
		$C_8H_{16} \rightarrow C_3H_6 + C_5H_{10}$	Positive
		$C_8H_{16} \rightarrow 2C_4H_8$	Negative
	1-Pentene	$C_5H_{10} \rightarrow C_2H_4 + C_3H_6$	Positive
		$2C_5H_{10} \rightarrow C_{10}H_{20}$	Positive
		$C_{10}H_{20} \rightarrow 2C_5H_{10}$	Negative

or propylene, and kinetic constant of considered reaction respectively. Eq. (9) obtained by combining sensitivity coefficient Eq. (8) with rate equation Eq. (1). Then, sensitivity coefficient value $|\sigma_{ij}|$, computed form sensitivity analysis Eq. (9) and for 5 reactions showed the maximum sensitivity a graphs were plotted, Fig. S2 and Fig. S3.

$$\frac{\partial \sigma_{i,j}}{\partial\left(\frac{W}{F_{0,feed}}\right)} = \frac{k_j}{\hat{X}_i}\frac{\partial}{\partial k_j}\sum_j \alpha_{j,i} r_j + \sum_l \frac{\partial \hat{y}_l}{\partial \hat{X}_l}\frac{\partial}{\partial \hat{y}_l}\sum_j \alpha_{j,i} r_j \sigma_{i,j} \quad (9)$$

Generally, it was observed that sensitivity was higher at short contact time for dominant reactions but for the longer the contact time the less influence among reactions observed.

A summary of reactions routes mainly affecting ethylene and propylene production were given in Table S1. Extent of influence solely depend on the feed type. For propylene feed the dimerization of propylene to hexene and the cracking of hexene to ethylene and butene showed sensitivity towards ethylene yield whereas the cracking of hexene to propylene showed negative sensitivity. This indicated that dimerization was the first step for propylene cracking to ethylene production and its dimer hexene might not go back to propylene because of high amount propylene feed in the system.

For 1-butene feed dimerization of 1-butene to C_8 intermediate route influenced both ethylene and propylene yield positively. As it was discussed earlier 1-butene was not directly cracked to ethylene. C_8 intermediate cracking to butenes negatively influenced propylene production but for ethylene the negative influence came from C_8 intermediate cracking to propylene and pentene which has positive influence for propylene production.

Direct 1-pentene cracking in to ethylene and propylene highly influenced the yield of both ethylene and propylene. Propylene prefers dimerization of 1-pentene to C_{10} intermediate which crack to C_3 and C_7. Ethylene preferred propylene consumption by the interaction of feed pentene with propylene to give C_8 intermediate that can cracked to ethylene and hexene.

There were two competent reactions for 1-hexene feed cracking either hexene to ethylene and butene or hexene to two moles of propylene. The former route positively influenced ethylene yield and negatively influenced propylene yield whereas the latter route influenced propylene yield positively and negatively influenced ethylene yield. In most of the cases, propylene and ethylene production routes were in competition.

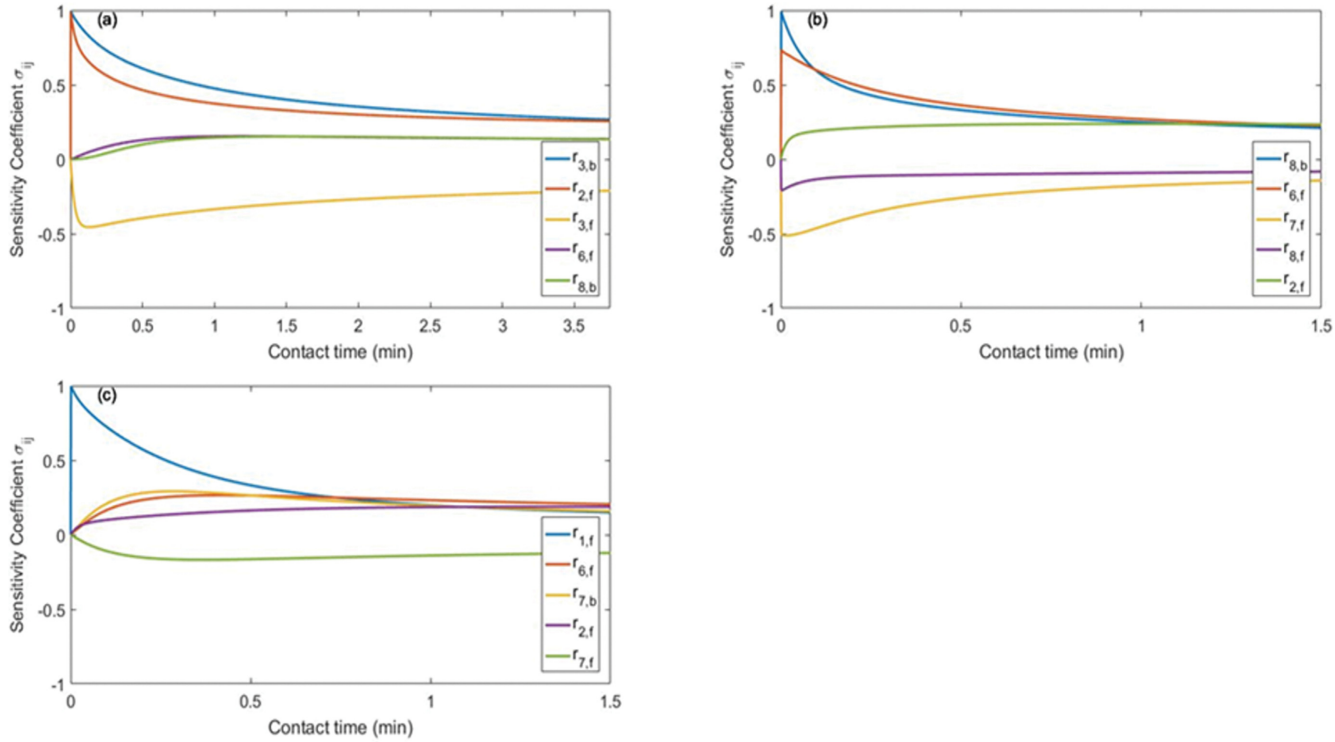

Fig. S3. Sensitivity analysis for ethylene yield from different feeds; (a) propylene, (b) 1-butene, and (c) 1-pentene.

REFERENCES

1. L. Ying, J. Zhu, Y. Cheng, L. Wang and X. Li, *J. Ind. Eng. Chem.*, **33**, 80 (2016).